

A model for the non-universal power-law of the solar wind sub-ion scale magnetic spectrum

T. Passot and P.L. Sulem

Laboratoire Lagrange,

Université Côte d'Azur, CNRS, Observatoire de la Côte d'Azur

CS 34229, 06304 Nice Cedex 4, France

passot@oca.eu; sulem@oca.eu

ABSTRACT

A phenomenological turbulence model for kinetic Alfvén waves in a magnetized collisionless plasma, able to reproduce the non-universal power-law spectra observed at the sub-ion scales in the solar wind and the terrestrial magnetosphere, is presented. The process of temperature homogenization along distorted magnetic field lines, induced by Landau damping, affects the turbulence transfer time and results in a steepening of the sub-ion power-law spectrum of critically-balanced turbulence, whose exponent is sensitive to the ratio between the Alfvén wave period and the nonlinear timescale. Transition from large-scale weak turbulence to smaller scale strong turbulence is captured and non local interactions, relevant in the case of steep spectra, are accounted for.

Subject headings: plasmas — turbulence — waves — magnetic fields — solar wind

1. Introduction

Spacecraft measurements both in the solar wind and the Earth magnetosphere (Bruno & Carbone 2013; Alexandrova et al. 2013, 2008a) show power-law energy spectra for magnetic turbulent fluctuations. At MHD scales, where kinetic effects are subdominant, observations support an Alfvénic energy cascade where the magnetic fluctuations transverse to the ambient field display a spectrum close to the $k_{\perp}^{-5/3}$ prediction based on a “critical balance” (Goldreich & Shridhar 1995; Nazarenko & Schekochihin 2011) between the characteristic times of the nonlinear transverse dynamics and of the Alfvén wave propagation along the magnetic field lines. At sub-ionic scales, a power law is also observed in a range extending from the proton (ρ_i) to the electron (ρ_e) Larmor radius (Sahraoui et al. 2009, 2010, 2011; Alexandrova et al. 2012; Chen et al. 2013), but the exponent appears to be less universal, with a distribution peaked near -2.8 and covering the interval $[-3.1, -2.5]$ (Fig. 5 of Sahraoui et al.

(2013)). For comparison, the magnetic spectral exponent in the MHD range is estimated as -1.63 ± 0.14 by Smith et al. (2006).

Gyrokinetic simulations at $\beta = 1$ display a sub-ion power-law spectrum with comparable exponents (-2.8 in Howes et al. (2011b) or -3.1 in Told et al. (2015)). Fully kinetic particle-in-cell (PIC) codes with a reduced mass ratio (Wan et al. 2015), as well as hybrid Eulerian Vlasov-Maxwell models (Servidio et al. 2015) also predict steep spectra at small scales, associated with coherent structures and deformation of the particle distribution functions.

At sub-ion scales, two types of waves play a dynamical role: whistlers for which ions are approximately cold and kinetic compressibility is negligible, and (low-frequency) kinetic Alfvén waves (KAWS) for which density fluctuations are significant. Reduced fluid-like models for the nonlinear dynamics of such waves have been developed and numerically simulated, leading to a $-8/3$ sub-ion spectral exponent (Schekochihin et al. 2009; Boldyrev & Perez 2012; Boldyrev et al. 2013;

Meyrand & Galtier 2013). Nevertheless a comprehensive understanding of turbulence at these scales is still missing. Carrying the critical-balance phenomenology to the KAW cascade leads to a $k_{\perp}^{-7/3}$ energy spectrum, significantly shallower than observed. Still assuming critical balance, Boldyrev et al. (2013) proposed a steeper spectrum resulting from coherent structures and intermittency corrections. Differently, Howes et al. (2008) suggested a balance between Landau damping and energy transfer. The $k_{\perp}^{-7/3}$ spectrum is then multiplied by an exponential factor originating from the variation of the energy flux along the cascade. This model was extended in Howes et al. (2011a), in an attempt to include nonlocal interactions, relevant for steep spectra.

In this letter we revisit KAW phenomenology, including in the energy transfer time the effect of ion temperature homogenization along magnetic field lines induced by Landau damping. The latter, whose linear rate is assumed to persist in the nonlinear regime (see Schekochihin et al. (2015) for a discussion), not only provides the exponential cut-off (at a scale depending on the Kolmogorov constant) discussed in Howes et al. (2006), but also leads to a steepening of the $-7/3$ power law. Furthermore, as it does not necessarily enforce strict critical balance, this model describes the transition between weak turbulence at large scales to strong turbulence at smaller scales.

2. Model setting

We consider a collisionless proton-electron plasma permeated by a strong ambient magnetic field (of amplitude B_0), with equal and isotropic mean temperatures $T_e = T_i$. Alfvén waves are driven in the MHD range, at scales much larger than ρ_i . The transverse magnetic field fluctuations δB_{\perp} are measured in velocity units by defining $b = v_A(\delta B_{\perp}/B_0)$, where v_A is the Alfvén velocity. The amplitude of these fluctuations at a transverse wavenumber k_{\perp} is $b_k \sim (k_{\perp} E_k)^{1/2}$, where E_k is the transverse magnetic spectrum.

2.1. Involved time scales

The magnetic field being stretched by electron velocity gradients and the dynamics dominantly transverse, we define, when the interactions are local, a stretching frequency (inverse of the non-

linear time τ_{NL}) $\omega_{NL} \sim k_{\perp} v_{ek}$ where the transverse electron velocity v_{ek} at scale k_{\perp}^{-1} is given by $v_{ek} = \bar{\alpha} b_k$. Here, $\bar{\alpha}$ is a function of $k_{\perp} \rho_i$, equal to 1 in the MHD range and scaling like $k_{\perp} \rho_i$ in the far sub-ion range, with a smooth transition near the ion gyroscale. As in hydrodynamic turbulence, we write $\omega_{NL} \sim [\bar{\alpha}^2 k_{\perp}^3 E_k]^{1/2}$ (Kovaszny 1948; Panchev 1969). Nevertheless, when E_k is decaying fast enough, the above expression does not necessarily ensure the expected monotonic growth of ω_{NL} . In this case nonlocal interactions cannot be neglected, and ω_{NL} should rather be viewed as the stretching rate due to all the scales larger than k_{\perp}^{-1} . It is then taken equal to the r.m.s. value $\omega_{NL} = \Lambda [\int_0^{k_{\perp}} \bar{\alpha}^2 p_{\perp}^2 E_p dp]^{1/2}$ (Elisson 1962; Panchev 1971; Lesieur 2008), where Λ is a constant. The local approximation is recovered when the integral diverges at large k_{\perp} , while the integral formula can be replaced by the equation $d\omega_{NL}^2/dk_{\perp} = \Lambda^2 \bar{\alpha}^2 k_{\perp}^2 E_k$.

Alfvén waves are characterized by a frequency $\omega_W = \bar{\omega} k_{\parallel} v_A$ and a dissipation rate $\gamma = \bar{\gamma} k_{\parallel} v_A$. Here $\bar{\omega}$ (equal to 1 in the MHD range) and $\bar{\gamma}$ are functions of $k_{\perp} \rho_i$ provided by the kinetic theory. In a linear description, parallel and perpendicular wavenumbers are defined relatively to the ambient field (taken in the z -direction), but distortions of the magnetic field lines should be retained in the nonlinear regime. We write $k_{\parallel} = k_z + v_A^{-1} [\int_0^{k_{\perp}} p_{\perp}^2 E_p dp]^{1/2}$, where k_z is a constant estimating the parallel wavenumber of the energy-containing Alfvén waves. It should not be confused with the inverse correlation length along the z -direction. Differently, k_{\parallel}^{-1} measures the correlation along the magnetic field lines (which is larger than along the z -axis). A procedure to estimate k_{\parallel} in numerical simulations is described in Cho & Lazarian (2004), while an approach using the frequency as a proxy for k_{\parallel} is used in TenBarge & Howes (2012). This suggests to write $\omega_W = \bar{\omega} k_z v_A + \delta\omega_W$ with a turbulent frequency shift $\delta\omega_W = [\int_0^{k_{\perp}} \bar{\omega}^2 p^2 E_p dp]^{1/2}$ or $d(\delta\omega_W)^2/dk_{\perp} = \bar{\omega}^2 k_{\perp}^2 E_k$. We similarly write $\gamma = \bar{\gamma} k_z v_A + \delta\gamma$ with $d(\delta\gamma)^2/dk_{\perp} = \bar{\gamma}^2 k_{\perp}^2 E_k$. A multiplicative constant should also enter the definitions of $\delta\omega_W$ and $\delta\gamma$, but is easily scaled out.

Another time scale originates from the compressible character of KAWs. The latter are subject to Landau damping, resulting in tempera-

ture homogenization along the magnetic field lines, on the correlation length k_{\parallel}^{-1} in a time $\tau_{Hr} \sim (v_{thr} k_{\parallel})^{-1}$. Here the thermal velocity v_{thr} appears as the r.m.s. streaming velocity of the r -particles. This time scale, which arises explicitly in Landau fluid closures (Hammett et al. 1997; Snyder et al. 1997; Sulem & Passot 2015), is very short for the electrons, while for the ions it is comparable to that of the other relevant processes and can thus affect the dynamics. Due to magnetic field distortion, this process introduces additional nonlinear couplings characterized by the frequency $\omega_H = \mu v_{thi} k_{\parallel}$ where μ is a numerical constant. We are thus led to write $\omega_H = \mu v_{thi} k_z + \delta\omega_H$ with $d(\delta\omega_H)^2/dk_{\perp} = \mu^2 \beta k_{\perp}^2 E_k$.

Finally, we define the transfer time $\tau_{tr} = \tau_{NL}(\tau_{NL}/\tau_W + \tau_{NL}/\tau_H)$, or in frequency terms $\omega_{tr} = \omega_{NL}^2/(\omega_W + \omega_H)$. When only one process competes with nonlinear stretching, the critical balance condition (Goldreich & Shridhar 1995; Nazarenko & Schekochihin 2011; Schekochihin et al. 2009) ensures the equality of the two associated time scales, and thus of the transfer and stretching times.

2.2. The nonlocal model

Retaining KAW linear Landau damping leads to the phenomenological equation (Howes et al. 2008, 2011a) $\partial_t E_k + \mathcal{T}_k = -2\gamma E_k + S_k$, where S_k is the driving term acting at large scales and \mathcal{T}_k the transfer term related to the energy flux ϵ by $\mathcal{T}_k = \partial\epsilon/\partial k_{\perp}$. Due to Landau damping, energy is not transferred conservatively along the cascade, making ϵ scale-dependent. For a steady state and outside the injection range, one has $d\epsilon/dk_{\perp} = -2\gamma E_k$. Note that the present setting differs from the asymptotic regime considered by Schekochihin et al. (2009) for which, under the simultaneous conditions $k_{\perp} \rho_i \gg 1$ and $k_{\perp} \rho_e \ll 1$, KAWs are not subject to Landau damping, as they transfer part of their energy via parallel phase mixing to the ion (electron) entropy cascades only at ion (electron) gyroscs, where it is cascaded both in physical and velocity spaces to collisional scales via perpendicular phase mixing.

Estimate of the energy flux relies on a basic turbulence description (overlooking intermittency). We write $\epsilon = C \omega_{tr} k_{\perp} E_k$, where C is a negative power of the Kolmogorov constant. Arguing that

the small-scale eddies cannot be sufficiently highly correlated with each other to contribute equally (Elisson 1962), we here use the local approximation $k_{\perp} E_k$ of the Reynolds stress rather than the original Obukhov's expression $\int_{k_{\perp}}^{\infty} E_p dp$ which leads to an unphysical behavior in the dissipation range of hydrodynamic turbulence (Panchev 1971).

Normalizing frequencies by Ω_i , wavenumbers by ρ_i^{-1} , energy spectra by $v_A^2 \rho_i$, energy fluxes by $v_A^2 \Omega_i$, and denoting by β the ion beta, we obtain the non-dimensional model equations (keeping the same notations)

$$d\omega_{NL}^2/dk_{\perp} = \Lambda^2 \beta^{-1} \bar{\alpha}^2 k_{\perp}^2 E_k \quad (1)$$

$$d(\delta\omega_W)^2/dk_{\perp} = \beta^{-1} \bar{\omega}^2 k_{\perp}^2 E_k \quad (2)$$

$$d(\delta\gamma)^2/dk_{\perp} = \beta^{-1} \bar{\gamma}^2 k_{\perp}^2 E_k \quad (3)$$

$$d(\delta\omega_H)^2/dk_{\perp} = \mu^2 k_{\perp}^2 E_k \quad (4)$$

$$d\epsilon/dk_{\perp} = -2[\beta^{-1/2} \bar{\gamma} k_z + (\delta\gamma)] E_k \quad (5)$$

$$E_k = [(\beta^{-1/2} \bar{\omega} + \mu) k_z + \delta\omega_W + \delta\omega_H] \frac{C^{-1} \epsilon}{k_{\perp} \omega_{NL}^2}. \quad (6)$$

Except possibly near $k_{\perp} = 1$, $\bar{\alpha} = \bar{\omega}$. The nonlinearity parameter $\chi = \omega_{NL}/\omega_W$ obeys

$$\frac{d\chi}{dk_{\perp}} = \frac{\bar{\alpha}^2 k_{\perp}^2 E_k}{2\beta \omega_{NL}^2} \chi \left(\Lambda^2 - \frac{\bar{\omega}^2}{\bar{\alpha}^2} \chi^2 \right) - k_z \frac{\chi^3}{2\omega_{NL}^2} f \quad (7)$$

where $f = \frac{2}{\sqrt{\beta}} \frac{d}{dk_{\perp}} (\bar{\omega} \delta\omega_W) + \frac{k_z}{\beta} \frac{d\bar{\omega}^2}{dk_{\perp}}$ is positive. At the (small) injection wavenumber k_0 , turbulence is characterized by $A = k_z/[k_0^3 E_{k_0}]^{1/2} = (k_z/k_0)(B_0/\delta B_{\perp 0})$ and, when taking $\omega_{NL}^{(0)} = \Lambda \beta^{-1/2} k_0^{3/2} E_{k_0}^{1/2}$ and $\omega_W^{(0)} = \beta^{-1/2} (k_z + k_0^{3/2} E_{k_0}^{1/2})$, $\chi_0 = \Lambda/(1+A)$. In the strong turbulence regime with $k_z = 0$, $\chi = \Lambda$ in the full spectral range, while for $k_z \neq 0$, χ starts growing near k_0 but cannot exceed Λ .

3. A simplified local-interaction model

3.1. The usual conservative cascades

Assuming local interactions, we have

$$E_k^2 \sim \frac{\beta^{1/2} \Lambda^{-2} C^{-1} \epsilon}{\bar{\alpha}^2 k_{\perp}^4} (\bar{\omega} + \mu \beta^{1/2}) (k_z + k_{\perp}^{3/2} E_k^{1/2}). \quad (8)$$

When neglecting dissipation (constant ϵ), we recover the usual inertial energy spectra. For weak

Λ	0.71	1	1.22	1.30	1.41	2	4.47
exponent	-3.18	-2.81	-2.69	-2.66	-2.63	-2.53	-2.45

Table 1: Sub-ion exponent versus Λ in conditions of Fig. 1a (fitting range $8 \leq k_\perp \leq 40$).

turbulence ($k_\perp^{3/2} E_k^{1/2} \ll k_z$), $E_k \propto k_\perp^{-2}$ in the MHD range, while in the sub-ion range (as $\bar{\omega} \gg \mu\beta^{1/2}$), $E_k \propto k_\perp^{-5/2}$. For strong turbulence (k_z negligible), $E_k \propto k_\perp^{-5/3}$ in the MHD range, while in the sub-ion range $E_k \propto k_\perp^{-7/3}$. A k_\perp^{-3} regime is also obtained in the sub-ion range when the effect of wave propagation is negligible, as observed in two-dimensional hybrid PIC simulations with an out-of-plane ambient magnetic field (Franci et al. 2015). Furthermore, as easily seen from eq. (6), an additional regime with $E_k \propto k_\perp^{-1}$ is possible at very large scales when, for small enough ϵ , turbulence is not yet developed and ω_{NL} almost constant. Such a spectral exponent is observed in the solar wind at scales larger than the $k_\perp^{-5/3}$ inertial range (Matthaeus & Goldstein 1986; Nicol et al. 2008; Wicks et al. 2010).

3.2. Effect of Landau damping

For strong turbulence, when assuming local interactions and neglecting k_z contributions,

$$\epsilon_k = \epsilon_0 \exp \left[-2C^{-1}\Lambda^{-2} \int_{k_0}^{k_\perp} \frac{\bar{\gamma}}{\xi \bar{\alpha}^2} (\bar{\omega} + \mu\beta^{1/2}) d\xi \right], \quad (9)$$

where the notation ϵ_k for the energy flux stresses its wavenumber dependence. This quantity is to be substituted in $E_k \sim \beta^{1/3} \Lambda^{-4/3} C^{-2/3} \epsilon_k^{2/3} k_\perp^{-7/3}$, taking $\bar{\alpha} = \bar{\omega}$ and $\bar{\gamma}/\bar{\omega}^2 \approx \delta(\beta)$ ($\approx 0.78\rho_e/\rho_i$ when using eqs. (62) and (63) of Howes et al. (2006) with $\beta = 1$). Furthermore, in this range $\bar{\omega} \approx a(\beta)k_\perp$ with $a(\beta) = (1 + \beta)^{-1/2}$. This leads to $\epsilon_k \sim \epsilon_0 k_\perp^{-\zeta} \exp(-2a(\beta)C^{-2}\Lambda^{-2}\delta(\beta)k_\perp)$, with $\zeta = 2\delta(\beta)C^{-1}\mu\Lambda^{-2}\beta^{1/2}$. This results in a steepening of the algebraic prefactor of the magnetic spectrum which is now proportional to $k_\perp^{-(7/3+2\zeta/3)} \exp[-(4/3)a(\beta)\delta(\beta)C^{-1}\Lambda^{-2}k_\perp]$. Compared with the spectrum obtained in Howes et al. (2008), the present model predicts that, in addition to an exponential cut-off, Landau damping leads to a correction of the power-law exponent. In contrast with intermittency corrections discussed in Boldyrev & Perez (2012), this correc-

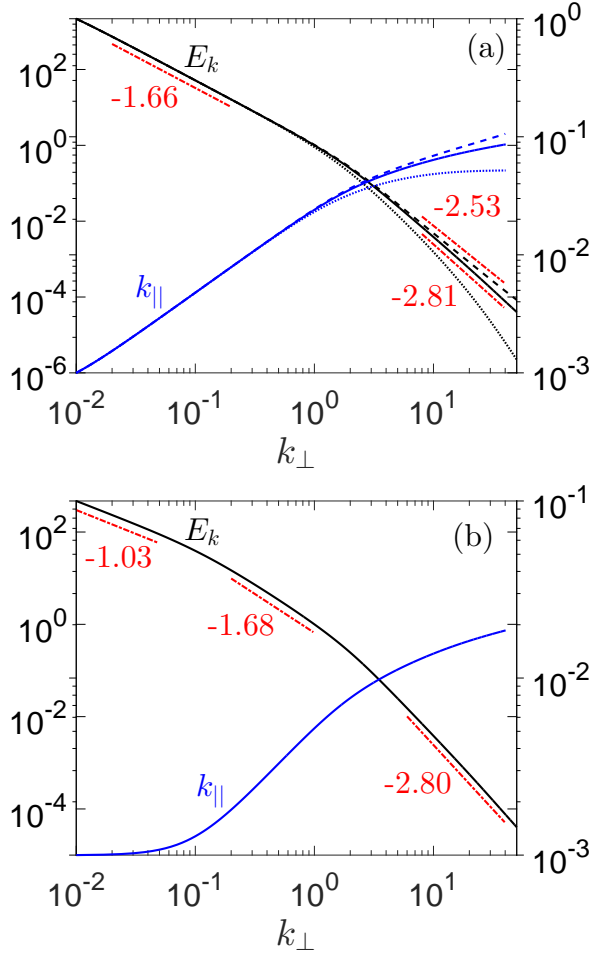


Fig. 1.— (a): Normalized energy spectrum E_k (black lines, l.h.s. labels and outer tickmarks) and parallel wavenumber k_\parallel (blue lines, r.h.s labels and inner tickmarks), for $k_z = 0$, $\beta = e = 1$ and $\Lambda = 2$ (dashed lines), 1 (solid lines) and 0.5 (dotted lines), (see other parameters in text); (b): Same as (a) for $\Lambda = 1$ and $\epsilon_0 = 10^{-2}$.

tion is not universal, which is expected when dissipation and nonlinear transfer times display the same wavenumber dependence (Bratanov et al. 2013). This situation holds for the second term in the exponential arising in eq. (9), that leads to the correction of the $-7/3$ spectral index. We note that it defines a dissipation length $k_d^{-1} = 2C^{-1}\Lambda^{-2}\mu\beta^{1/2}\bar{\gamma}/(k_\perp\bar{\alpha}^2) \propto k_\perp^{-1}$ and thus a dissipation rate $\omega_d = v_e k_d$ for ϵ_k , which has the same k_\perp dependency as ω_{NL} that, by a critical balance argument, identifies with ω_{tr} beyond the transition range. A similar power law decay of ϵ is encountered in drift-kinetic plasma turbulence (see eq. (2.53) of Schekochihin et al. (2015)).

Differently, for weak turbulence, we get

$$\epsilon_k = \left[\epsilon_0^{\frac{1}{2}} - \Lambda^{-1}C^{-\frac{1}{2}}\beta^{-\frac{1}{4}}k_z^{\frac{3}{2}} \int_{k_0}^{k_\perp} \frac{\bar{\gamma}}{\xi^2\bar{\alpha}^{\frac{1}{2}}} d\xi \right]^2, \quad (10)$$

where the integral behaves like $k_\perp^{1/2}$. Equation (10) predicts that ϵ_k and thus E_k vanish at a finite k_\perp , indicating the breaking of the analysis near the corresponding scale, an effect possibly related to the difficulty for weak turbulence to exist in the presence of a significant Landau damping.

4. Numerical integration of the full model

When the spectrum is too steep, a numerical integration of differential equations (1)-(6) is needed. The functions $\bar{\omega}$ and $\bar{\gamma}$ are then evaluated from the full linear kinetic theory by means of the WHAMP software (Rönnmark 1982). Moreover, $\bar{\alpha} = \bar{\omega}$. We prescribed conditions at $k_\perp = k_0$ in the form $\omega_{NL}^{(0)} = \Lambda\beta^{-1/2}\bar{\alpha}_{k_0}k_0^{3/2}E_0^{1/2}$, $\delta\omega_W^{(0)} = \beta^{-1/2}\bar{\omega}_{k_0}k_0^{3/2}E_0^{1/2}$, $\delta\gamma^{(0)} = \beta^{-1/2}\bar{\gamma}_{k_0}k_0^{3/2}E_0^{1/2}$, $\delta\omega_H^{(0)} = \mu k_0^{3/2}E_0^{1/2}$ and $\epsilon_0 = eCk_0\omega_{NL}^{(0)2}E_0/[(\beta^{-1/2}\bar{\omega} + \mu)k_z + \delta\omega_W + \delta\omega_H]$. Here E_0 is an arbitrary constant (taken equal to 1 with no lack of generality). We chose $k_0 = 10^{-2}$, $C = 1.25$ and $\mu = 1.8$. Except when otherwise specified, we also took $e = 1$. For clarity's sake, when several energy spectra are plotted in the same panel, one of them (solid line) is normalized by its value at $k_\perp = 1$, while the others (dashed and dotted lines) are rescaled to make all the spectra equal at $k_\perp = k_0$. In red are indicated the fitting ranges (dashed-dotted straight lines) and the corresponding spectral exponents whose last

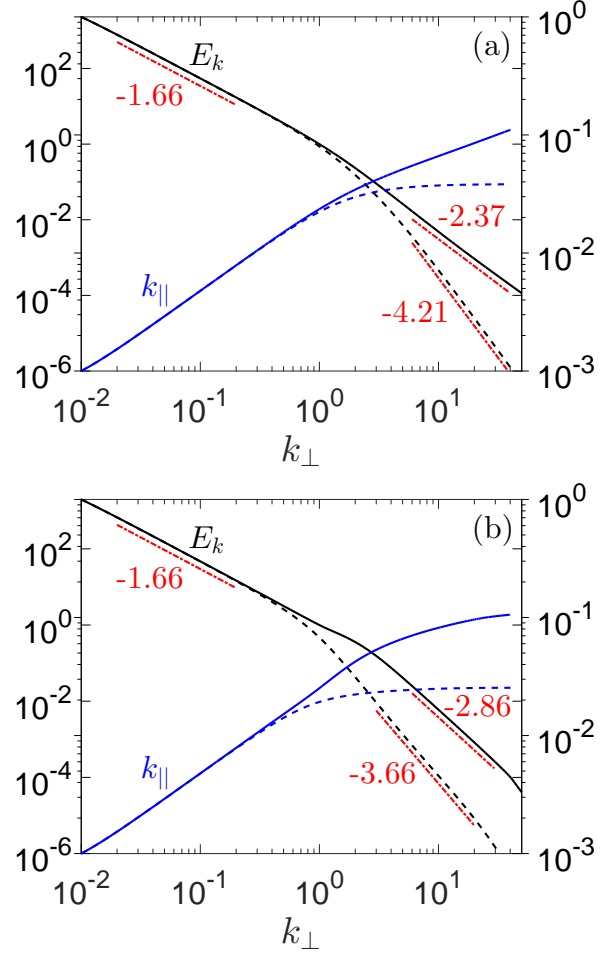


Fig. 2.— Same as Fig. 1a with $\beta = 0.01$, $\Lambda = 1$ (solid lines) and 0.45 (dashed lines) (a), and $\beta = 10$, $\Lambda = 3.16$ (solid lines) and 1 (dashed lines) (b).

digit only is sensitive to moderate changes of the fitting domain.

In Fig. 1a, we focus on the strong turbulence regime for $\beta = 1$, assuming $k_z = 0$. In the MHD range, a $k_\perp^{-5/3}$ energy spectrum establishes and k_\parallel scales like $k_\perp^{2/3}$ in all the cases. Differently, at the sub-ion scales, the spectrum is steeper when Λ is smaller, displaying exponents -2.53 for $\Lambda = 2$, -2.81 for $\Lambda = 1$, and a fast decay for $\Lambda = 0.5$. In this range, k_\parallel increases slower, and this even more so when Λ is smaller. In the present setting, $\Lambda \approx 0.71$ (leading to a spectral exponent -3.18) and $\Lambda \approx 4.47$ (exponent -2.45) appear as the extreme values for existence of an extended power-law spectrum at the sub-ion scales. These limit exponents are consistent with the dispersion of solar-wind measurements. Exponents for intermediate values of Λ are displayed in Table 1. Their statistical distribution (and the most probable value) are nevertheless beyond the scope of the model. Note that a $-7/3$ exponent (rarely reported in observations) is approached for large Λ , only when $\mu = 0$.

When keeping $\Lambda = 1$ but decreasing the energy transfer rate ϵ_0 by taking $e = 10^{-2}$ (Fig. 1b), the MHD and sub-ion spectral exponents are not affected, but a k_\perp^{-1} range becomes visible at the largest scales. In this range, where k_\parallel remains small, turbulence is not developed, possibly as in the solar wind energy containing range. Further decrease of ϵ_0 leads to a k_\perp^{-1} range extending down to the ion gyroscale, a situation observed in the magnetosheath near the bow shock (Czaykowska et al. 2001; Alexandrova et al. 2008b).

Another issue is the influence of β , keeping $k_z = 0$. For $\beta = 0.01$ (Fig. 2a), we considered $\Lambda = 1$ and $\Lambda = 0.45$, leading to sub-ion spectral exponents -2.37 and -4.21 respectively, while as expected the MHD range is not affected. For $\beta = 10$ (Fig. 2b), we used $\Lambda = 3.16$ and 1 , for which the sub-ion exponents are -2.86 and -3.66 respectively. For the former value of Λ , a spectral bump is visible in the transition zone, consequence of the sharp decrease of the ion Landau damping at these scales (see e.g. Fig. 3 of Howes et al. (2006)).

To justify the chosen values of Λ (which is equal to χ in the above setting where $k_z = 0$

and prescribes its saturated value when $k_z \neq 0$), it should be noted that, at a fixed wavenumber, χ increases with the amplitude of the fluctuations, linearly in weak turbulence and at a slower rate when the amplitude gets larger, a behavior supported by FLR-Landau fluid simulations (in preparation). Furthermore, the Mach number, which scales like $b_0\beta^{-1/2}$ (where b_0 measures the amplitude of the large-scale turbulent fluctuations) is usually observed to be moderate in the solar wind (Bavassano & Bruno 1995), in spite of the broad range of reported values of β (Chen et al. 2014). This implies that the turbulence level, and thus Λ , should be decreased at smaller β .

Figure 3 addresses the influence of the parameter A when Λ is fixed at a moderate value, here $\sqrt{2}$. Increasing A results in a change from strong to weak turbulence near the driving scale. For $A = 0.5$ (Fig. 3a), the function χ rapidly saturates to a value slightly smaller than Λ , establishing critical balance and thus a strong turbulence regime. The spectral exponent -1.72 measured in the MHD range differs from $-5/3$, since χ is still in the growing phase, but choosing k_0 smaller would ensure a $k_\perp^{-5/3}$ critically-balanced MHD range. At small scales, the exponent is -2.62 , comparable to the values displayed in Fig. 1a. The case $A = 5$ corresponds to an intermediate regime where χ_0 is significantly smaller, resulting in a -1.92 large-scale spectrum, steeper than $-5/3$ but nevertheless distinguishable from the -2 weak-turbulence value. The sub-ion exponent -2.71 is consistent with a strong turbulence regime, characterized by an almost constant χ at these scales. In Fig. 3b, $A = 10$ and 15 , both lead to a weak-turbulence regime at large scales, with exponents -1.95 and -1.97 , very close to the theoretical value. Differences nevertheless hold at small scales. For $A = 10$, the sub-ion dynamics corresponds to strong turbulence, qualitatively similar to the case $A = 5$, with a spectral exponent -2.9 and an almost constant χ , although somewhat smaller. Differently, for $A = 15$, the fluctuations are too weak for the energy transfer to efficiently compete with Landau damping, leading to an exponential decay of sub-ion spectrum, and a function χ which starts to decrease by $k_\perp\rho_i = 10$.

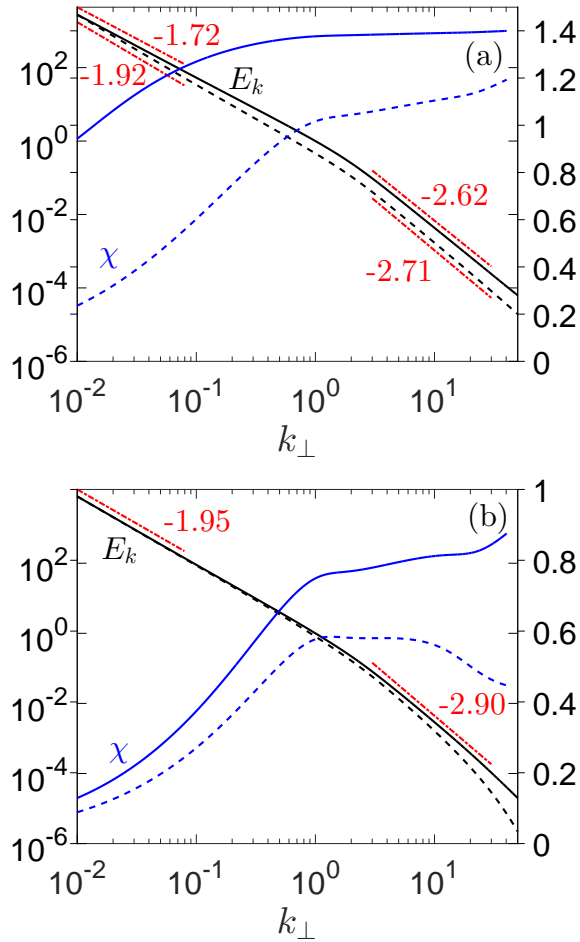


Fig. 3.— (a): Energy spectrum E_k (l.h.s. labels) and nonlinear parameter χ (r.h.s. labels) for $\Lambda = \sqrt{2}$ with $A = 0.5$ (solid lines) and $A = 5$ (dashed lines); (b): Same as (a), with $A = 10$ (solid lines) and $A = 15$ (dashed lines).

5. Conclusion

This model predicts a non-universal power-law spectrum for strong turbulence at the sub-ion scales (beyond the transition range) with an exponent which, in contrast with the $-5/3$ inertial MHD cascade, depends on the saturation level of the nonlinearity parameter χ , covering a range of values consistent with solar wind and magnetosheath observations. Such a non universality, associated with Landau damping, was also reported in three-dimensional PIC simulations of whistler turbulence (Gary et al. 2012) and FLR-Landau fluid simulations of KAW turbulence (in preparation). As the present approach does not capture sub-electron scale dynamics, the exponential cut-off might be replaced by another regime, such as the steep power laws reported from both numerical simulations (Camporeale & Burgers 2011; Gary et al. 2012) and spacecraft data (Sahraoui et al. 2013).

The research leading to these results has received funding from the European Commission's Seventh Framework Programme (FP7/2007-2013) under the grant agreement SHOCK (project number 284515).

REFERENCES

- Alexandrova, O., Chen, C. H. K., Sorriso-Valvo, L., Horbury, T. S., & Bale, S. D. 2013, *Space Sci. Rev.*, 178, 102
- Alexandrova, O., Lacombe, C., & Mangeney, A. 2008a, *Ann. Geophys.*, 26, 35853596
- . 2008b, *Ann. Geophys.*, 26, 3585
- Alexandrova, O., Lacombe, C., Mangeney, A., Grappin, R., & Maksimovic, M. 2012, *Astrophys. J.*, 760, 121
- Bavassano, B., & Bruno, R. 1995, *J. Geophys. Res.*, 100 (A6), 9475
- Boldyrev, S., Horaites, K., Xia, Q., & Perez, J. C. 2013, *Astrophys. J.*, 777, 41
- Boldyrev, S., & Perez, J. C. 2012, *Astrophys. J. Lett.*, 758, L44
- Bratanov, V., Jenko, F., Hatch, D. R., & Wilczek, M. 2013, *Phys. Rev. Lett.*, 111, 075001

- Bruno, R., & Carbone, V. 2013, *Living Rev. Solar Phys.*, 10
- Camporeale, E., & Burgers, D. 2011, *Astrophys. J.*, 730, 114
- Chen, C. H. K., Boldyrev, S., Xia, Q., & Perez, J. C. 2013, *Phys. Rev. Lett.*, 110, 225002
- Chen, C. H. K., Leung, L., Boldyrev, S., Maruca, B. A., & Bale, S. D. 2014, *Geophys. Res. Lett.*, 41, 8081
- Cho, J., & Lazarian, A. 2004, *Astrophys. J.*, 615, L41
- Czaykowska, A., Bauer, T. M., Treumann, R. A., & Baumjohann, W. 2001, *Ann. Geophys.*, 19, 275
- Elisson, T. H. 1962, in *Coll. Intern. du CNRS*, Vol. 108, *Mécanique de la turbulence* (Marseilles, August 28-Sept. 2, 1961), ed. A. Fabre, 113–119
- Franci, L., Verdini, A., Matteini, L., Landi, S., & Hellinger, P. 2015, *Astrophys. J. Lett.*, 804, L39
- Gary, S. P., Chang, O., & Wang, J. 2012, *Astrophys. J.*, 755, 142
- Goldreich, P., & Shridhar, S. 1995, *Astrophys. J.*, 438, 763
- Hammett, G. W., Dorland, W., & Perkins, F. W. 1997, *Phys. Fluids B*, 4, 2052
- Howes, G. G., Cowley, S. C., Dorland, W., & Hammett, G. W. 2006, *Astrophys. J.*, 651, 590
- Howes, G. G., Cowley, S. C., Dorland, W., et al. 2008, *J. Geophys. Res.*, 113, A05105
- Howes, G. G., TenBarge, J. M., & Dorland, W. 2011a, *Phys. Plasmas*, 18, 102305
- Howes, G. G., TenBarge, J. M., Dorland, W., et al. 2011b, *Phys. Rev. Lett.*, 107, 035004
- Kovaszny, L. S. G. 1948, *J. Aeron. Sc.*, 12, 745
- Lesieur, M. 2008, *Fluid Mechanics and Applications*, Vol. 84, *Turbulence in fluids* (Springer)
- Matthaeus, W. H., & Goldstein, M. L. 1986, *Phys. Rev. Lett.*, 57, 495
- Meyrand, R., & Galtier, S. 2013, *Phys. Rev. Lett.*, 111, 264501
- Nazarenko, S. V., & Schekochihin, A. A. 2011, *J. Fluid Mech.*, 677, 134
- Nicol, R. M., Chapman, S. C., & Dendy, D. O. 2008, *Astrophys. J.*, 679, 862
- Panchev, S. 1969, *Phys. Fluids*, 12, 935
- . 1971, *Random functions and turbulence* (Pergamon Press, Oxford)
- Rönnmark, K. 1982, *Waves in homogeneous, anisotropic multicomponent plasmas* (WHAMP), Tech. Rep. 179, Kiruna Geophysical Institute
- Sahraoui, F., Goldstein, M. L., Belmont, G., Canu, P., & Rezeau, L. 2010, *Phys. Rev. Lett.*, 105, 131101
- Sahraoui, F., Goldstein, M. L., Robert, P., & Khotyaintsev, Y. V. 2009, *Phys. Rev. Lett.*, 102, 231102
- Sahraoui, F., Huang, S. Y., Belmont, G., et al. 2013, *Astrophys. J.*, 777, 11
- Sahraoui, F., Goldstein, M. L., Belmont, G., et al. 2011, *Planet. Space Sc.*, 59, 585
- Schekochihin, A. A., Cowley, S. C., Dorland, W., et al. 2009, *Astrophys. J. Suppl.*, 182, 310
- Schekochihin, A. A., Parker, J. T., Highcock, E. G., et al. 2015, eprint arXiv:1508.05988
- Servidio, S., Valentini, F., Perrone, D., et al. 2015, *J. Plasma Phys.*, 81, 325810107
- Smith, C. W., Hamilton, K., Vasquez, B. J., & Leamon, R. J. 2006, *Astrophys. J. Lett.*, 645, L85
- Snyder, P. B., Hammett, G. W., & Dorland, W. 1997, *Phys. Plasmas*, 4, 3974
- Sulem, P. L., & Passot, T. 2015, *J. Plasma Phys.*, 81(1), 325810103
- TenBarge, J. M., & Howes, G. G. 2012, *Phys. Plasmas*, 18, 055902

- Told, D., Jenko, F., TenBarge, J. M., Howes, G. G., & Hammett, G. 2015, Phys. Rev. Lett., 115, 025003
- Wan, M., Matthaeus, W. H., Roytershteyn, V., et al. 2015, Phys. Rev. Lett., 114, 175002
- Wicks, R. T., Horbury, T. S., Chen, C. H. K., & Schekochihin, A. A. 2010, Mon. Not. R. Astron. Soc., 407, L31